THE JOURNAL OF BIOLOGICAL CHEMISTRY VOL. 290, NO. 6, pp. 3784–3792, February 6, 2015

Loss of Apoptosis Regulator through Modulating IAP Expression (ARIA) Protects Blood Vessels from Atherosclerosis*

Received for publication, August 15, 2014, and in revised form, December 16, 2014 Published, JBC Papers in Press, December 22, 2014, DOI 10.1074/jbc.M114.605287

Kiyonari Matsuo[‡], Yoshiki Akakabe[‡], Youhei Kitamura[‡], Yoshiaki Shimoda[‡], Kazunori Ono[‡], Tomomi Ueyama[‡], Satoaki Matoba[‡], Hiroyuki Yamada[‡], Kinta Hatakeyama[§], Yujiro Asada[§], Noriaki Emoto[¶], and Koji Ikeda[¶1]

From the [‡]Department of Cardiology, Graduate School of Medical Science, Kyoto Prefectural University of Medicine, 465 Kajii, Kawaramachi-Hirokoji, Kamigyo, Kyoto 602-8566, the [¶]Department of Clinical Pharmacy, Kobe Pharmaceutical University, 4-19-1 Motoyama-Kitamachi, Higashinada, Kobe 6588558, and the [§]Department of Pathology, Faculty of Medicine, University of Miyazaki, Miyazaki 889-1692, Japan

Background: Macrophages play central roles in the whole process of atherosclerosis.
Results: ARIA regulates macrophage foam cell formation at least in part by modulating ACAT-1 expression.
Conclusion: ARIA is a novel factor involved in the pathogenesis of atherosclerosis.
Significance: Loss of ARIA ameliorated atherosclerosis by reducing macrophage foam cell formation; inhibition of ARIA may represent a new line of therapy against atherosclerosis.

Atherosclerosis is the primary cause for cardiovascular disease. Here we identified a novel mechanism underlying atherosclerosis, which is provided by ARIA (apoptosis regulator through modulating IAP expression), the transmembrane protein that we recently identified. ARIA is expressed in macrophages present in human atherosclerotic plaque as well as in mouse peritoneal macrophages. When challenged with acetylated LDL, peritoneal macrophages isolated from ARIA-deficient mice showed substantially reduced foam cell formation, whereas the uptake did not differ from that in wild-type macrophages. Mechanistically, loss of ARIA enhanced PI3K/Akt signaling and consequently reduced the expression of acyl coenzyme A:cholesterol acyltransferase-1 (ACAT-1), an enzyme that esterifies cholesterol and promotes its storage, in macrophages. Inhibition of PI3K abolished the reduction in ACAT-1 expression and foam cell formation in ARIA-deficient macrophages. In contrast, overexpression of ARIA reduced Akt activity and enhanced foam cell formation in RAW264.7 macrophages, which was abrogated by treatment with ACAT inhibitor. Of note, genetic deletion of ARIA significantly reduced the atherosclerosis in ApoE-deficient mice. Oil red-O-positive lipid-rich lesion was reduced, which was accompanied by an increase of collagen fiber and decrease of necrotic core lesion in atherosclerotic plaque in ARIA/ApoE double-deficient mice. Analysis of bone marrow chimeric mice revealed that loss of ARIA in bone marrow cells was sufficient to reduce the atherosclerogenesis in ApoE-deficient mice. Together, we identified a unique role of ARIA in the pathogenesis of atherosclerosis at least partly by modulating macrophage foam cell formation. Our results indicate that ARIA could serve as a novel pharmacotherapeutic target for the treatment of atherosclerotic diseases.

Atherosclerosis has prevailed for ~4,000 years of human history and is the primary cause of cardiovascular disease, which is the leading cause of death in industrialized society (1–3). Chronic inflammation plays a fundamental role in atherosclerosis, and macrophages are crucially involved in the whole process of atherosclerosis from an early fatty streak lesion to the rupture of advanced plaque (4, 5). Macrophages contribute to the local inflammatory response in the subendothelial space by producing cytokines and also play a pivotal role in the lesion remodeling and plaque rupture by producing metalloproteinases (5). Moreover, macrophages accumulate cholesterol esters and consequently form lipid-laden foam cells, which are hallmarks of atherosclerogenesis (6, 7).

Atherogenic lipoproteins are ingested by macrophages through scavenger receptors such as SR-A (scavenger receptor class A) and CD36 and delivered to the late endosome/lysosome, where cholesterol esters are hydrolyzed into free cholesterol and fatty acids (4, 7). A fraction of free cholesterol undergoes re-esterification and is subsequently stored in cytoplasmic lipid droplets, which are catalyzed by acyl coenzyme A:cholesterol acyltransferase-1 (ACAT-1)[2] in macrophages (4, 7). Accordingly, ACAT-1 plays a central role in macrophage foam cell formation; therefore, inhibiting ACAT-1 has been considered a fascinating approach for the prevention and/or treatment of atherosclerosis. However, the role of ACAT-1 inhibition in preventing atherosclerosis has remained controversial. Systemic deletion of ACAT-1 modestly reduced atherosclerotic lesion formation without reducing plasma cholesterol levels in LDL-deficient mice (8). In contrast, ACAT-1 deletion in macrophages increased atherosclerosis in association with enhanced apoptosis of macrophages in the plaque (9). Pharmaco-

* This work was supported by Grant-in-aid for Scientific Research C: KAKENHI-23591107 and Grants-in-aid for Challenging Exploratory Research KAKENHI-23659423 and -26670406, as well as a research grant from Takeda Science Foundation.
[1] To whom correspondence should be addressed: Tel.: 81-78-441-7537; Fax: 81-75-441-7538; E-mail: ikedak-circ@umin.ac.jp.

[2] The abbreviations used are: ACAT, acyl coenzyme A:cholesterol acyltransferase; ARIA, apoptosis regulator through modulating IAP expression; IAP, inhibitor of apoptosis; PTEN, phosphatase and tensin homolog deleted on chromosome 10; PM, peritoneal macrophage; BMC, bone marrow cell; HCD, high-cholesterol diet; DKO, double knock-out; NS, not significant.

logical inhibition of ACAT-1 showed different effects on atherosclerosis in animal models depending on chemical compound (10–12). Finally, recent clinical trials of ACAT inhibitors for the treatment of atherosclerosis showed negative results, yet some beneficial effects on inflammation and endothelial function have also been reported (13–16). Nevertheless, inhibition of ACAT-1 is still an attractive antiatherogenic strategy because it could ameliorate atherosclerosis *in situ* independent of the serum cholesterol levels; therefore, it may reduce the remaining risk in patients treated with cholesterol-lowering drugs such as statins.

Recently, crucial roles of Akt in the progression of atherosclerosis have been reported. Loss of Akt1 leads to severe atherosclerosis by increasing inflammatory mediators and reducing endothelial NO synthase (eNOS) phosphorylation in vessel walls, suggesting that the vascular origin of Akt1 exerts vascular protection against atherogenesis (17). On the other hand, Akt3 deficiency promotes atherosclerosis by enhancing macrophage foam cell formation because of increased ACAT-1 expression, suggesting that the macrophage origin of Akt3 is important to prevent atherosclerosis (18). Therefore, Akt differentially modifies the process of atherosclerosis.

We previously identified a transmembrane protein, named apoptosis regulator through modulating IAP expression (ARIA), that modulates PI3K/Akt signaling (19). ARIA binds to phosphatase and tensin homolog deleted on chromosome 10 (PTEN), an endogenous antagonist for PI3K, and enhances levels of membrane-associated PTEN (20). Because membrane localization is a major determinant for PTEN activity, ARIA enhances PTEN function, leading to inhibition of PI3K/Akt signaling (19, 20). ARIA is highly expressed in endothelial cells; therefore, loss of ARIA substantially enhanced angiogenesis by accelerating endothelial PI3K/Akt signaling. Moreover, we found a significant role of ARIA in the fine-tuning of PI3K/Akt signaling in cardiomyocytes (21). ARIA deficiency protects the heart from doxorubicin-induced cardiac dysfunction by reducing cardiomyocyte death due to enhanced cardiac PI3K/Akt signaling.

In this study, we identified a previously unknown role of ARIA in the pathogenesis of atherosclerosis. Genetic loss of ARIA reduced atherosclerosis, and this atheroprotective effect of ARIA deletion was likely macrophage-dependent. Mechanistically, ARIA-mediated modification of PI3K/Akt signaling regulates ACAT-1 expression in macrophages, and thus modulates macrophage foam cell formation in atherosclerotic lesions. Our data suggest that ARIA is a novel pharmacotherapeutic target for the prevention and/or treatment of cardiovascular diseases.

EXPERIMENTAL PROCEDURES

Materials—Antibodies for phospho-Akt (Ser-473) and total-Akt were obtained from Cell Signaling Technology. Antibody for GAPDH was obtained from Millipore, and the FLAG-M2 antibody was obtained from Sigma. Anti-mouse CD68 antibody was obtained from Santa Cruz Biotechnology. Antibody for human ARIA (ECSM2) was obtained from Everest Biotech. Antibody for human CD68 was obtained from Dako. Unlabeled or Alexa Fluor 488-labeled acetylated LDL was obtained from Life Technologies. LY294002 and ACAT inhibitor (Sandoz 58-035) were obtained from Sigma.

Cell Culture—RAW264.7 cells, a murine macrophage cell line, were cultured in DMEM supplemented with 10% FBS. For overexpression of ARIA, RAW cells were transfected with ARIA cDNA subcloned into p3×FLAG-CMV-14 (Sigma) or empty vector using Lipofectamine 2000 (Invitrogen) when they reached ~70% confluency. Fresh growth medium was given 24 h after transfection, and cells were further cultured for 24 h, followed by protein extraction. At the time of protein extraction, both cells transfected with ARIA-FLAG or empty vector were nearly confluent, and no significant difference of confluency was detected between the groups. Murine peritoneal macrophages (PMs) were prepared as described previously (22). Briefly, thioglycolate (2 ml of 3% solution in water) was intraperitoneally injected in age- and sex-matched WT and ARIA-deficient mice. After 3–4 days, sterile ice-cold PBS was injected into the cavity of each mouse, followed by gentle massage and fluid collection. Cells were collected by centrifugation at 1,000 rpm for 6 min and then resuspended in RPMI 1640 medium supplemented with 10% FBS. The cells were plated in 6-well tissue culture plates at a density of 5.0×10^6 cells/well. After a 2-h incubation to allow adherence, non-adherent cells were removed by washing wells with prewarmed RPMI 1640 medium, and the adhered macrophages were cultured. The culture media were replaced every other day, and the macrophages were used for the experiments within 5 days after harvesting.

Foam Cell Formation—Foam cell formation was performed as described previously (22, 23). Briefly, macrophages were cultured on chamber slides at a density of 5.0×10^5 cells/well and treated with acetylated LDL (60 mg/ml) for 48 h in the presence or absence of either LY294002 (5 μM) or ACAT inhibitor (5 μM). Cells were then stained with oil red-O to detect the lipid accumulation. The oil red-O-positive area was measured using the ImageJ software, and at least 5 fields and 100 cells per condition were analyzed. Quantification of macrophage foam cells was performed by calculating the mean oil red-O-positive area per cells. To analyze the uptake of acetylated LDL, macrophages were treated with Alexa Fluor 488-labeled acetylated LDL (60 mg/ml) for 24 h. Subsequently, cellular uptake of acetylated LDL was quantitatively analyzed using a fluorescence microplate reader (Infinite 200 PRO, TECAN).

Human Autopsy Material—Human coronary arteries were obtained from autopsy cases after informed consent was provided by their families. The clinical investigation conformed to the principles outlined in the Declaration of Helsinki and was approved by the Ethical Committee of the University of Miyazaki.

Preparation of Retrovirus—To prepare retroviruses, cDNAs for target genes (ARIA-FLAG or ACAT-1-FLAG) were subcloned into pMSCVneo vector (Clontech). GP2-293 packaging cells were transfected with these pMSCVneo plasmids and pVSV-G plasmid (Clontech) using Lipofectamine 2000. In parallel, GP2-293 cells were transfected with empty pMSCVneo and pVSV-G plasmids to prepare viruses for negative control. Fresh growth medium was given 24 h after transfection, and cells were further cultured for 24 h, followed by collection of the virus-containing culture medium. For infection, PMs of ~50% confluency were incubated in the virus-containing medium in the presence of 8 μg/ml Polybrene for 24 h. Subsequently, cells

were given fresh growth medium and cultured for 24 h, followed by protein extraction. Cells reached ~80% confluency at the time of harvest, and no significant difference of confluency between groups was observed.

Immunoblotting—Immunoblotting was performed as reported previously (24). Briefly, cells were lysed with radioimmunoprecipitation assay buffer containing protease and phosphatase inhibitors, followed by protein quantification using DC protein assay kit (Bio-Rad). Cell lysates containing the same amount of proteins were subjected to SDS-polyacrylamide gel electrophoresis, followed by transferring onto the nitrocellulose membranes. The membranes were blocked with 5% nonfat milk in TBS containing 0.05% Tween 20 at room temperature for 1 h. Membranes were then incubated with the appropriate antibody to detect target molecules at 4 °C for overnight. Subsequently, membranes were incubated with secondary antibody, and the signals were detected using ECL Western blotting detection kit (GE Healthcare).

Immunohistochemistry—Serial sections of human coronary arteries were prepared, followed by deparaffinization. Sections then underwent blocking with 5% normal donkey serum and 5% bovine serum albumin in PBS following antigen retrieval using protease K. After blocking with hydrogen peroxide and blocking reagent for avidin/biotin (Vector Laboratories), sections were incubated with blocking reagent (negative), anti-human ARIA (1:300), or anti-human CD68 (1:80) at 4 °C for overnight. Signals were detected using ImmPACT 3,3′-diaminobenzidine (Vector Laboratories) following the reaction with biotinylated secondary antibodies and VECTASTAIN ABC system (Vector Laboratories). For fluorescent double staining, sections were incubated with anti-goat IgG antibody conjugated with Alexa Fluor 488 and anti-mouse IgG antibody conjugated with Alexa Fluor 594 after incubation with anti-human ARIA and anti-human CD68 antibodies, followed by signal detection under fluorescent microscopy.

Quantitative PCR—Quantification of mRNA expression of target genes was performed as reported previously (25). Briefly, total RNA was extracted from cells or tissues using TRIzol (Invitrogen), followed by purification with the RNeasy MinElute cleanup kit (Qiagen). Complementary DNA was synthesized from ~1 μg of total RNA using the PrimeScript RT reagent kit with gDNA Eraser (TaKaRa, Shiga, Japan). PCR reactions were prepared using SYBR Premix Ex Taq II (TaKaRa), followed by quantitative PCR on Thermal Cycler Dice (TaKaRa). The nucleotide sequence of each primer is shown in Table 1.

Atherosclerotic Lesion Analysis—All experimental protocols were approved by the Ethics Review Committee for Animal Experimentation of the Kyoto Prefectural University of Medicine. Mice were fed with a high-cholesterol diet containing 16.5% fat and 1.25% cholesterol (Oriental Yeast, Tokyo, Japan) for 15 weeks. For en face analysis, the entire aorta from the heart, extending 5 mm after bifurcation of the iliac arteries and including the subclavian right and left common carotid arteries, was removed, dissected, and stained with oil red-O. The oil red-O-positive atherosclerotic lesion area was measured using the ImageJ software. For the analysis of the atherosclerotic lesion at the aortic sinus, serial cryosections were prepared from the region of the proximal aorta through the aortic sinuses, and then either stained with oil red-O, hematoxylin, or Masson's trichrome or immunostained with an anti-CD68 antibody.

TABLE 1
Nucleotide sequence of primers

Mouse ARIA	ATGTCCTTCAGCCACAGAAGCACAC CACGTTGATGTTCCTCATGGAGATG
ACAT-1-FLAG-specific	GAAGCATTCAGTGTGGTTGTACTA TTTGTAGTCAGCCCGGGATCC
Endogenous ACAT-1-specific	GCTCCTAAGGCTCCAGAAGCTGGCT CACAGCAGGTCCTTCTGACACACCA
ACAT-1-common	CTCAGCACGATCGTCGTGGACTACA AGAGCAAGCCATGGACAAGGGAATAG
ABCA1	ATCGTGTCTCGCCTGTTCTCAGACG CGCCTGCAGCAGGCTGTCCACAGTA
ABCG1	GTCCAACCGAGTCACCAAGGAGGCCTC GCACTGTCTGCATTGCGTTGCATTGC
Actin	CTCTCAGCTGTGGTGGTGAA AGCCATGTACGTAGCCATCC

Bone Marrow Transplantation—Bone marrow transplantation was performed as described previously (20). Briefly, bone marrow cells (BMCs) were isolated from the femurs of ApoE/ARIA double-deficient or ApoE-deficient mice, and 5×10^6 cells per body of BMCs were transfused into recipient mice that received 8 grays of lethal irradiation. Four weeks after BMC transplantation, high-cholesterol diet feeding was initiated and continued for 12 weeks, and then blood vessels were harvested.

Statistics—Differences between groups were analyzed using the Student's *t* test or one-way analysis of variance with post hoc multiple comparison using Bonferroni's/Dunn's test. $p < 0.05$ was considered statistically significant. Data are presented as mean ± S.E.

RESULTS

ARIA Regulates PI3K/Akt Signaling in Macrophages—Macrophages play a central role in the pathogenesis of atherosclerosis. We previously found modest expression of ARIA in murine macrophage cell line PU5-1.8 (19); therefore, ARIA expression in primary mouse PM was examined. PMs expressed ARIA at a level similar to that in mouse aortic endothelial cells, whereas murine macrophage cell line RAW264.7 exhibited minimal ARIA expression (Fig. 1*A*).

We then examined whether ARIA is expressed in macrophages in human atherosclerotic plaque using immunohistochemistry. Significant ARIA staining was detected in endothelial cells, which is consistent with its high expression in endothelial cells (Fig. 1*B*). Of note, CD68-positive macrophages present in human plaque appeared to be positive for ARIA (Fig. 1*B*). Some of the ARIA-positive cells in the plaque were negative for CD68, suggesting that cells other than macrophages may also express ARIA in atherosclerotic plaque. We also confirmed the ARIA expression in CD68-positive macrophages by immunofluorescent double staining (Fig. 1*C*).

Furthermore, we found that ARIA expression in the aorta of ApoE-deficient mice significantly increased during a high-cholesterol diet (HCD) feeding as compared with that during a normal chow feeding (Fig. 1*D*). These results suggest that ARIA

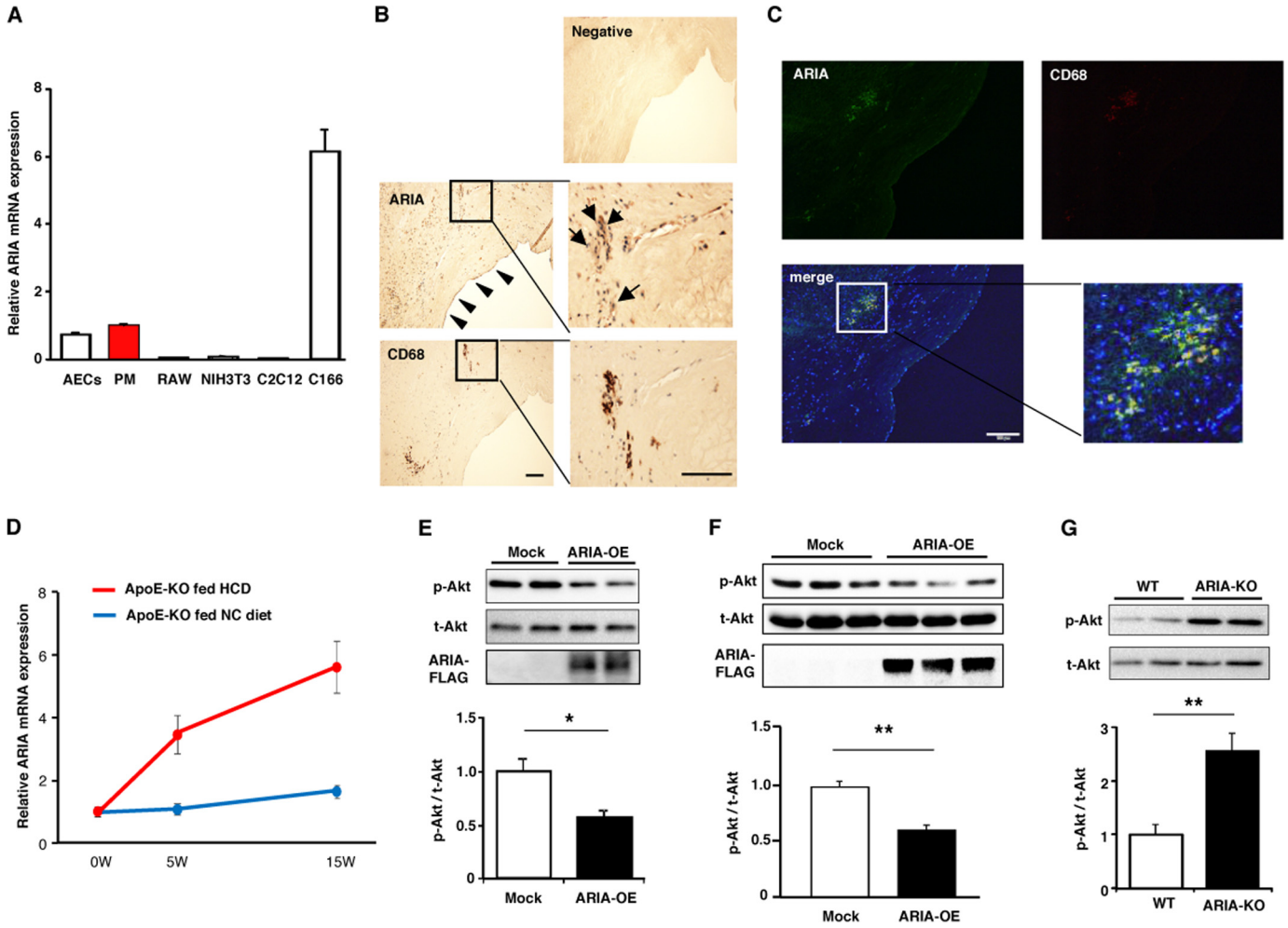

FIGURE 1. **ARIA regulates PI3K/Akt signaling in macrophages.** *A*, quantitative analysis of ARIA mRNA expression. ARIA was expressed in mouse PMs at a level comparable with mouse aortic endothelial cells (*AECs*). RAW, NIH3T3, and C2C12 are cell lines for mouse macrophages, fibroblasts, and myoblasts, respectively. Highest expression was detected in mouse endothelial cell line, C166 ($n = 3$ each). *B*, immunohistochemistry for ARIA and CD68 in human atherosclerotic plaque. ARIA staining was detected in endothelial cells as indicated by *arrowheads*. CD68-positive macrophages appear to be positive for ARIA staining (*arrows*). *Bar*: 100 μm. *C*, immunofluorescent staining for ARIA (*green*) and CD68 (*red*) in human atherosclerotic plaque. Most of the CD68-positive macrophages are also positive for ARIA. *Bar*: 100 μm. *D*, expression of ARIA in the aortas of ApoE-deficient mice fed either HCD or normal chow (*NC*) for the indicated duration ($n = 4$ each). *E*, immunoblotting for Akt and ARIA-FLAG. Akt activity was significantly reduced in RAW macrophages overexpressing ARIA (*ARIA-OE*). *, $p < 0.05$ ($n = 8$ each). *F*, immunoblotting for Akt and ARIA-FLAG. Akt activity was significantly reduced in PMs overexpressing ARIA (*ARIA-OE*). **, $p < 0.01$ ($n = 9$ each). *G*, immunoblotting for Akt. PMs isolated from ARIA-deficient mice ($ARIA^{-/-}$) showed significantly enhanced Akt activity as compared with that in WT macrophages. *p-Akt*, phospho-Akt; *t-Akt*, total Akt. **, $p < 0.01$ ($n = 6$ each). *Error bars* in *A* and *D–G* indicate mean ± S.E.

has a potential role in the development of atherosclerosis by modulating macrophage functions.

We previously reported that ARIA regulates PI3K/Akt signaling in endothelial cells and cardiomyocytes in a cell-autonomous fashion (20, 21). Therefore, we examined whether ARIA regulates PI3K/Akt signaling in macrophages as well. Overexpression of ARIA significantly reduced phosphorylation of Akt in RAW264.7 macrophages (Fig. 1*E*). Overexpression of ARIA in PMs also reduced Akt phosphorylation (Fig. 1*F*), whereas genetic loss of ARIA significantly enhanced Akt phosphorylation in PMs (Fig. 1*G*). These results strongly suggest that ARIA also regulates PI3K/Akt signaling in macrophages in a cell-autonomous manner.

ARIA Modulates Macrophage Foam Cell Formation—Recently, the crucial role of Akt3 in the regulation of macrophage foam cell formation has been reported. Akt3 accelerates the degradation of ACAT-1 that catalyzes the esterification of free cholesterols for storage into cytoplasmic lipid droplets. Accordingly, loss of Akt3 enhanced macrophage foam cell formation by increasing ACAT-1 expression. Because ARIA regulates PI3K/Akt signaling in macrophages, we explored whether ARIA modulates macrophage foam cell formation. PMs isolated from WT and $ARIA^{-/-}$ mice exhibited a similar uptake of acetylated LDL (Fig. 2*A*). Nevertheless, PMs isolated from $ARIA^{-/-}$ mice showed a significant reduction in foam cell formation as compared with PMs from WT mice (Fig. 2*B*). Inhibition of PI3K abolished the reduction in foam cell formation in PMs from $ARIA^{-/-}$ mice, suggesting that loss of ARIA reduced foam cell formation by enhancing PI3K/Akt signaling in PMs (Fig. 2*C*).

We then examined whether ARIA modifies ACAT-1 expression in macrophages. Because all the commercially available antibodies for ACAT-1 we used failed to detect endogenous ACAT-1 in PMs in our experiments, we analyzed the expression levels of retrovirus-mediated recombinant ACAT-1-FLAG in PMs. Genetic loss of ARIA caused a significant reduction in ACAT-1-FLAG protein expression in PMs, whereas

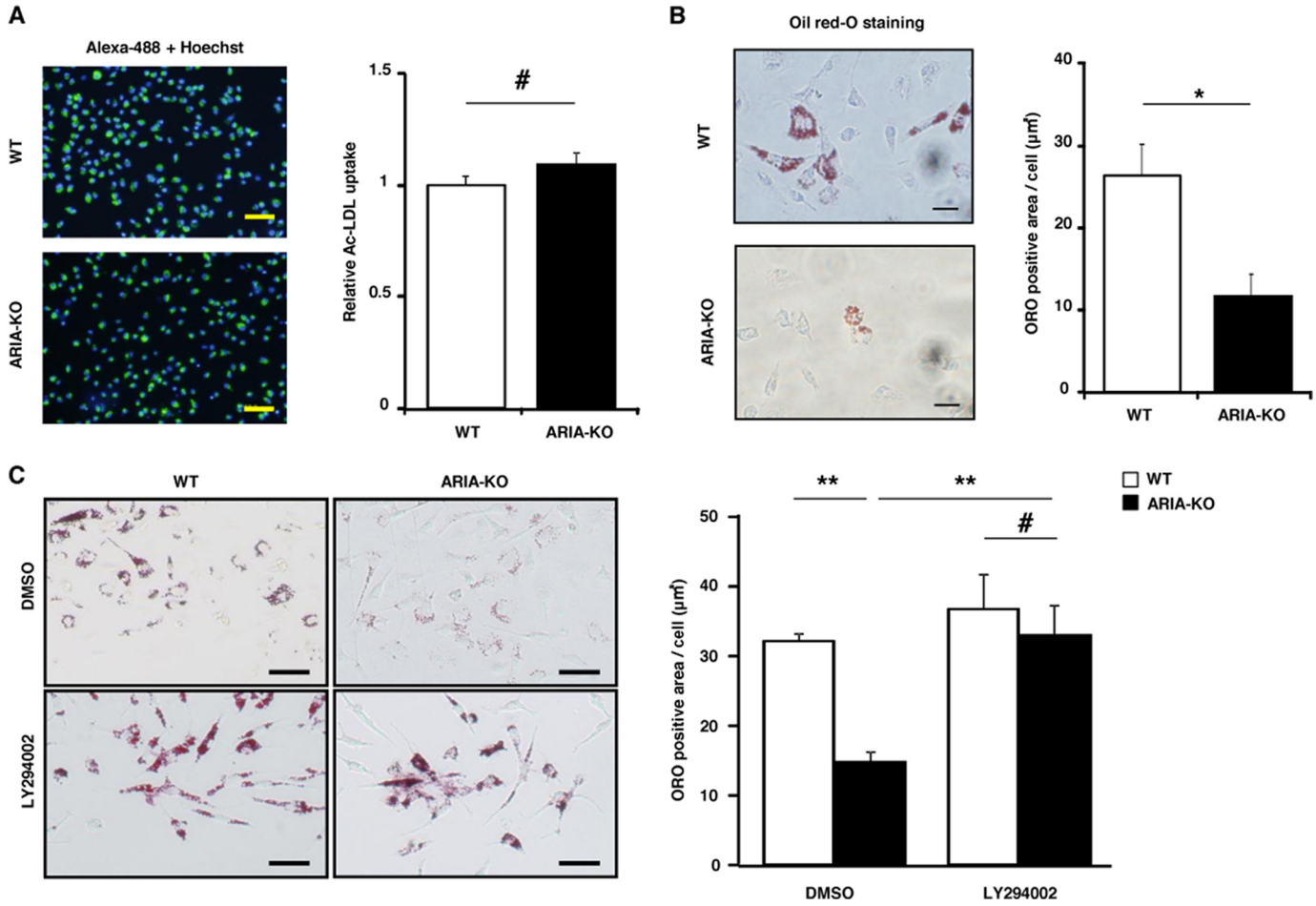

FIGURE 2. **ARIA regulates macrophage foam cell formation.** *A*, quantitative analysis of the uptake of acetylated LDL. PMs isolated from WT or ARIA$^{-/-}$ mice were treated with acetylated LDL conjugated with Alexa Fluor 488. Uptake of acetylated LDL was similar in PMs isolated from either WT or ARIA$^{-/-}$ mice. *Bar*: 50 μm. #, NS ($n = 12$ each). *B*, foam cell formation assay. PMs isolated from WT or ARIA$^{-/-}$ mice were treated with acetylated LDL, and their foam cell formation was evaluated by oil red-O (*ORO*) staining. PMs from ARIA$^{-/-}$ mice showed significantly reduced foam cell formation as compared with that in PMs of WT mice. *, $p < 0.05$ ($n = 4$ each). *Bar*: 20 μm. *C*, foam cell formation of PMs. Treatment with PI3K inhibitor (LY294002) abolished the reduced foam cell formation in PMs from ARIA$^{-/-}$ mice. *DMSO*, dimethyl sulfoxide. **, $p < 0.01$ and #, NS ($n = 6$ each). *Bar*: 20 μm. *Error bars* in all panels indicate mean ± S.E.

mRNA expression of ACAT-1-FLAG was similar between PMs isolated from WT and ARIA$^{-/-}$ mice (Fig. 3, *A* and *B*). We also confirmed that endogenous ACAT-1 mRNA as well as total ACAT-1 mRNA (includes both endogenous and exogenous mRNA) levels were similar between PMs isolated from WT and ARIA$^{-/-}$ mice (Fig. 3*B*). Moreover, inhibition of PI3K abolished the reduction of ACAT-1-FLAG protein expression observed in PMs from ARIA$^{-/-}$ mice (Fig. 3*A*). We further investigated the turnover of recombinant ACAT-1-FLAG expressed in PMs from WT or ARIA$^{-/-}$ mice. ACAT-1-FLAG degradation was significantly accelerated in ARIA$^{-/-}$ PMs as compared with that in WT PMs (Fig. 3, *C* and *D*). Of note, inhibition of PI3K abrogated the accelerated degradation of ACAT-1-FLAG in ARIA$^{-/-}$ PMs (Fig. 3, *C* and *D*). These results strongly suggest that genetic loss of ARIA reduces ACAT-1 protein expression in PMs by accelerating its degradation due to enhanced PI3K/Akt signaling.

Overexpression of ACAT-1 significantly enhanced foam cell formation in RAW264.7 macrophages (Fig. 3*E*). Notably, ARIA overexpression enhanced foam cell formation as well as ACAT-1 overexpression, and this ARIA-mediated increase in foam cell formation was abolished by the ACAT inhibitor (Fig. 3*E*). These data collectively indicate that ARIA modulates macrophage foam cell formation by modifying ACAT-1 expression through modulating PI3K/Akt signaling in macrophages. Additionally, we observed that loss of ARIA did not affect the expression of genes regulating cholesterol efflux such as ABCA-1 and ABCG-1, which is consistent with the previous study indicating that Akt3 does not modulate the cholesterol efflux in macrophages (18).

Genetic Loss of ARIA Reduces Atherosclerosis—To analyze the role of ARIA in atherosclerosis *in vivo*, we generated ARIA/ApoE double knock-out (DKO) mice and fed them with an HCD. DKO mice exhibited significantly reduced atherosclerotic lesions as assessed by en face quantification of aorta as compared with ApoE$^{-/-}$ mice (Fig. 4*A*). Histological analysis of atherosclerotic plaques at the aortic sinus revealed that the oil red-O-positive lipid area in the plaques was significantly reduced in DKO mice as compared with ApoE$^{-/-}$ mice, whereas macrophage infiltration in plaques assessed by CD68 immunostaining did not differ between these groups of mice (Fig. 4, *B* and *C*). Moreover, collagen content assessed by Masson's trichrome staining increased and the necrotic core area decreased in the plaques of DKO mice as compared with

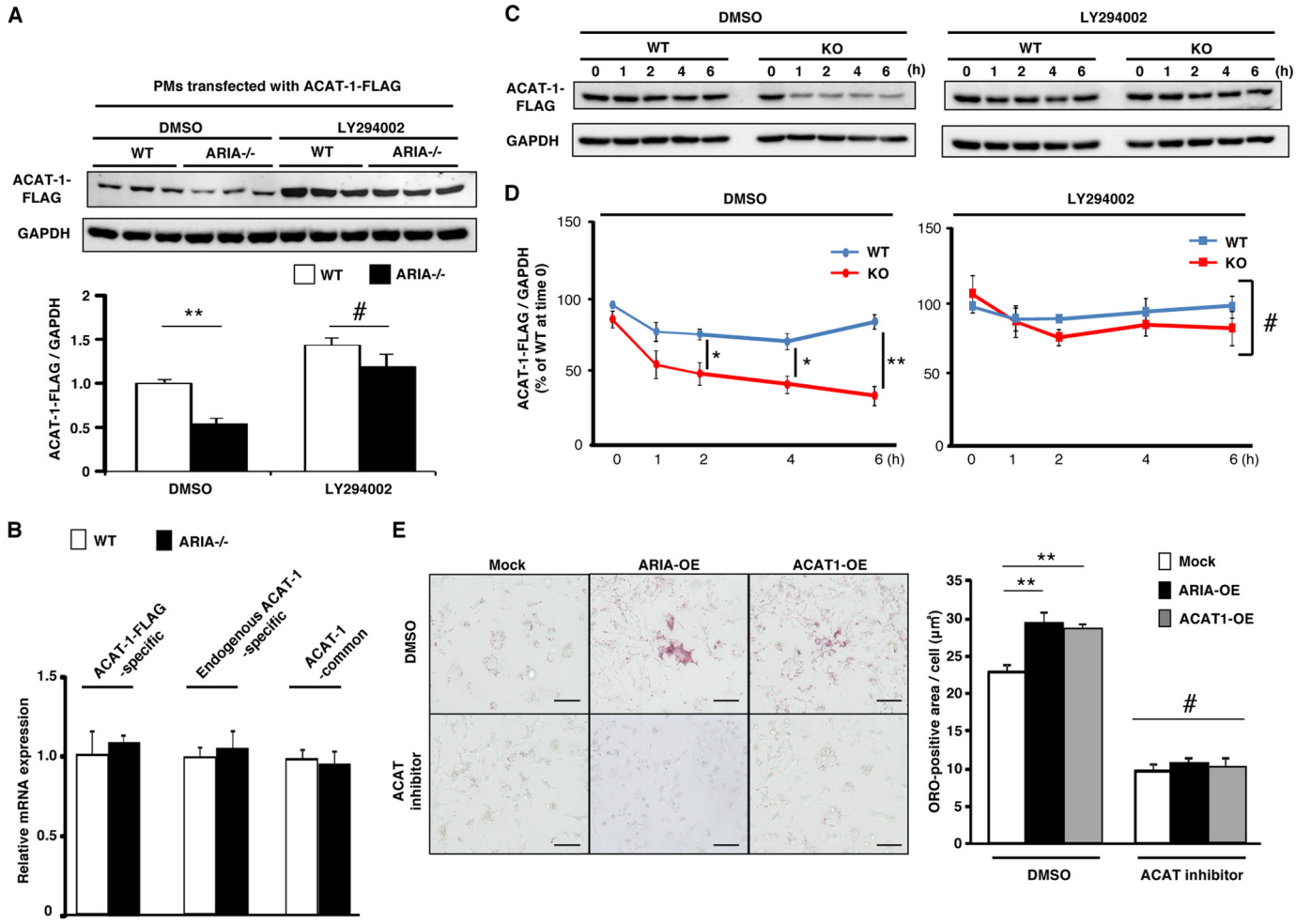

FIGURE 3. **ARIA regulates ACAT-1 expression in macrophages.** *A*, immunoblotting for ACAT-1-FLAG. PMs isolated from ARIA$^{-/-}$ mice exhibited reduced protein expression of ACAT-1-FLAG as compared with PMs of WT mice. **, $p < 0.01$ *versus* PMs of WT ($n = 6$ each). Of note, inhibition of PI3K by LY294002 abolished the reduction of ACAT-1 in PMs from ARIA$^{-/-}$ mice. *DMSO*, dimethyl sulfoxide. *B*, mRNA expression of ACAT-1 was not different between PMs isolated from WT or ARIA-KO mice ($n = 8$ each). *C*, cycloheximide chase assay for recombinant ACAT-1-FLAG. PMs isolated from WT or ARIA$^{-/-}$ mice were infected with ACAT-1-FLAG retrovirus and then treated with cycloheximide (50 μg/ml) in the presence or absence of PI3K inhibitor (LY294002; 5 μM) for the indicated times. Expression of ACAT-1-FLAG was analyzed by immunoblotting. *D*, cycloheximide chase assay. Quantitative analysis of ACAT-1-FLAG is shown. Degradation of ACAT-1-FLAG was significantly accelerated in PMs from ARIA$^{-/-}$ mice. *, $p < 0.05$ and **, $p < 0.01$ ($n = 4$ each). Inhibition of PI3K by LY294002 abolished the accelerated degradation of ACAT-1-FLAG in ARIA$^{-/-}$ macrophages. #, NS ($n = 4$ each). *E*, foam cell formation assay in RAW macrophages transfected with ARIA (*ARIA-OE*) or ACAT-1 (*ACAT1-OE*). ARIA-OE cells showed enhanced foam cell formation, as did ACAT1-OE cells. **, $p < 0.01$ ($n = 6$ each). Treatment with ACAT inhibitor completely abolished the enhanced foam cell formation in ARIA-OE cells as well as in ACAT1-OE cells. #, NS among groups. *Bar*: 50 μm. *Error bars* in *A*, *B*, *D*, and *E* indicate mean ± S.E.

ApoE$^{-/-}$ mice (Fig. 4, *D* and *E*). Serum lipid profiles were similar between DKO and ApoE$^{-/-}$ mice fed an HCD for 15 weeks (Fig. 4*F*). Similar to PMs from ARIA$^{-/-}$ mice, PMs from DKO mice showed significantly reduced foam cell formation when challenged with acetylated LDL as compared with PMs from ApoE$^{-/-}$ mice (data not shown). Furthermore, resident PMs isolated from ARIA$^{-/-}$ mice fed an HCD exhibited significantly reduced foam cell formation as compared with resident PMs from HCD-fed ApoE$^{-/-}$ mice (Fig. 4*G*). These data strongly suggest that loss of ARIA ameliorated atherosclerosis by reducing macrophage foam cell formation.

Atheroprotective Effects of ARIA Deletion Depend on Bone Marrow Cells—We previously reported that ARIA is highly expressed in endothelial cells and modulates endothelial PI3K/Akt signaling (19, 20). Because Akt1 in blood vessels has a protective role in the progression of atherosclerosis (17), we investigated whether ARIA deficiency in macrophages is indeed atheroprotective, by performing bone marrow transplantation experiments. Successful bone marrow transplantation was confirmed by genotyping of BMCs and tails of recipient mice (Fig. 5*A*). ApoE$^{-/-}$ mice harboring DKO BMCs showed significantly reduced atherosclerosis, whereas DKO mice transplanted with ApoE$^{-/-}$ (ARIA$^{+/+}$) BMCs exhibited no significant change in atherosclerotic lesions as compared with control ApoE$^{-/-}$ mice transplanted with ApoE$^{-/-}$ BMCs (Fig. 5*B*). Lipid accumulation was significantly reduced and collagen content increased in plaques of ApoE$^{-/-}$ mice having DKO BMCs as compared with control ApoE$^{-/-}$ mice (Fig. 5*C*). In contrast, DKO mice transplanted with ApoE$^{-/-}$ BMCs exhibited lipid accumulation and collagen content in plaques at a level similar to that in control ApoE$^{-/-}$ mice (Fig. 5*C*). These data suggest that loss of ARIA in BMCs but not endothelial cells plays a major role in the reduced atherosclerosis observed in DKO mice.

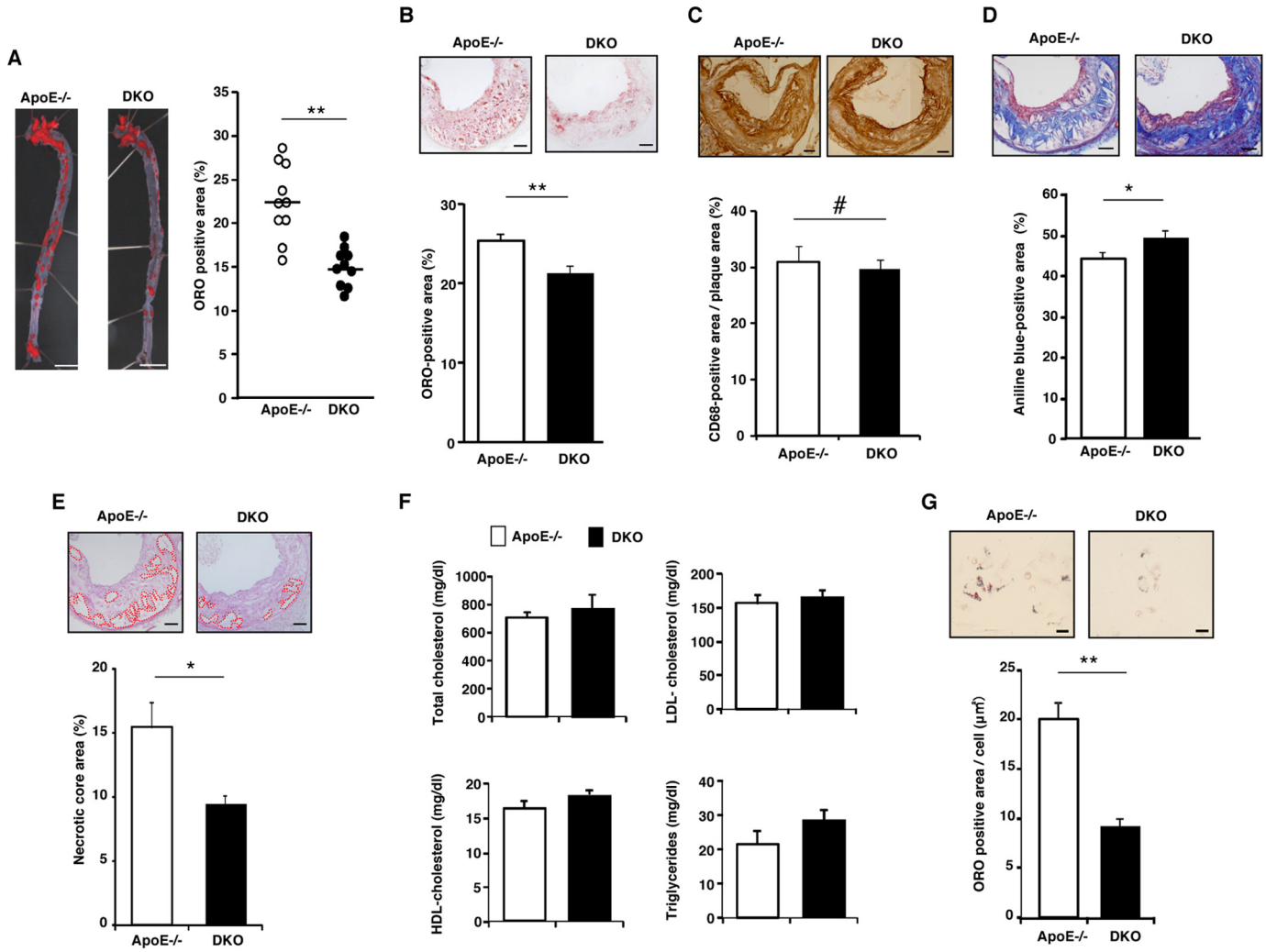

FIGURE 4. **Genetic loss of ARIA reduces atherosclerosis.** *A*, en face preparation of aorta stained with oil red-O (*ORO*). ARIA and ApoE DKO mice showed significantly reduced atherosclerotic lesion. **, $p < 0.01$ ($n = 10$ each). *Bar*: 5 mm. *B*, histology of plaques at the aortic sinus stained with oil red-O. Oil red-O-positive lipid-rich lesion was significantly reduced in the plaques of DKO mice. **, $p < 0.01$ ($n = 13$ each). *Bar*: 100 μm. *C*, histology of plaques at the aortic sinus immunostained with anti-CD68 antibody. Macrophage content in plaques at the aortic sinus was not different between ApoE$^{-/-}$ and DKO mice. #, NS ($n = 5$ each). *Bar*: 100 μm. *D*, histology of plaques at the aortic sinus stained with Masson's trichrome. Collagen fibers were significantly increased in the plaques of DKO mice. *, $p < 0.05$ ($n = 15$ each). *Bar*: 100 μm. *E*, histology of plaques at the aortic sinus stained with hematoxylin and eosin. Necrotic core was significantly reduced in the plaques of DKO mice. *, $p < 0.05$ ($n = 10$ each). *Bar*: 100 μm. *F*, serum lipid profiling of ApoE$^{-/-}$ or DKO mice fed a high cholesterol-diet for 15 weeks. Levels of serum cholesterol and triglycerides were similar between ApoE$^{-/-}$ and DKO mice ($n = 10$ each). *G*, foam cell formation of resident PMs isolated from ApoE$^{-/-}$ or DKO fed an HCD. Resident PMs from DKO mice fed an HCD showed significantly reduced foam cell formation. **, $p < 0.01$ ($n = 10$ each). *Error bars* in all panels indicate mean ± S.E.

DISCUSSION

Atherosclerosis results from the excessive lipid accumulation and chronic inflammation in vessel walls and involves various cells, including endothelial cells, vascular smooth muscle cells, and macrophages (2). Macrophages especially play a fundamental role in the progression of atherosclerosis by initiating inflammation and the formation of lipid-laden foam cells (5, 7). Inhibition of foam cell formation is a fascinating approach for the prevention of atherosclerosis because it could directly inhibit the atherosclerosis *in situ* independent of the control of other risk factors such as serum cholesterol levels and impaired glucose homeostasis. ACAT-1 plays a pivotal role in foam cell formation by catalyzing the esterification of free cholesterols for storage into cytoplasmic lipid droplets (5, 8), suggesting that inhibition of ACAT-1 may be beneficial in preventing atherosclerosis. However, loss of ACAT-1 in macrophages unexpectedly worsened atherosclerosis, probably because of the increase in cytotoxic free cholesterol in macrophages. These results indicate that partial and/or moderate inhibition of ACAT-1 in macrophages may be important in eliciting its beneficial effects on atherosclerosis; therefore, detailed molecular mechanisms underlying the regulation of ACAT-1 expression need to be elucidated for the development of ideal ACAT-1 inhibitor.

Recently, the crucial role of Akt3 in the degradation of ACAT-1 in macrophages has been reported (18). Akt3 potentially phosphorylates ACAT-1, which initiates ACAT-1 polyubiquitylation and subsequent proteasomal degradation. Akt3 deficiency in macrophages promoted foam cell formation and atherosclerosis in ApoE$^{-/-}$ mice, suggesting that Akt-mediated degradation of ACAT-1 protects vessel walls from atherosclerosis (18). In this study, we identified that ARIA negatively regulates PI3K/Akt signaling and consequently modulates

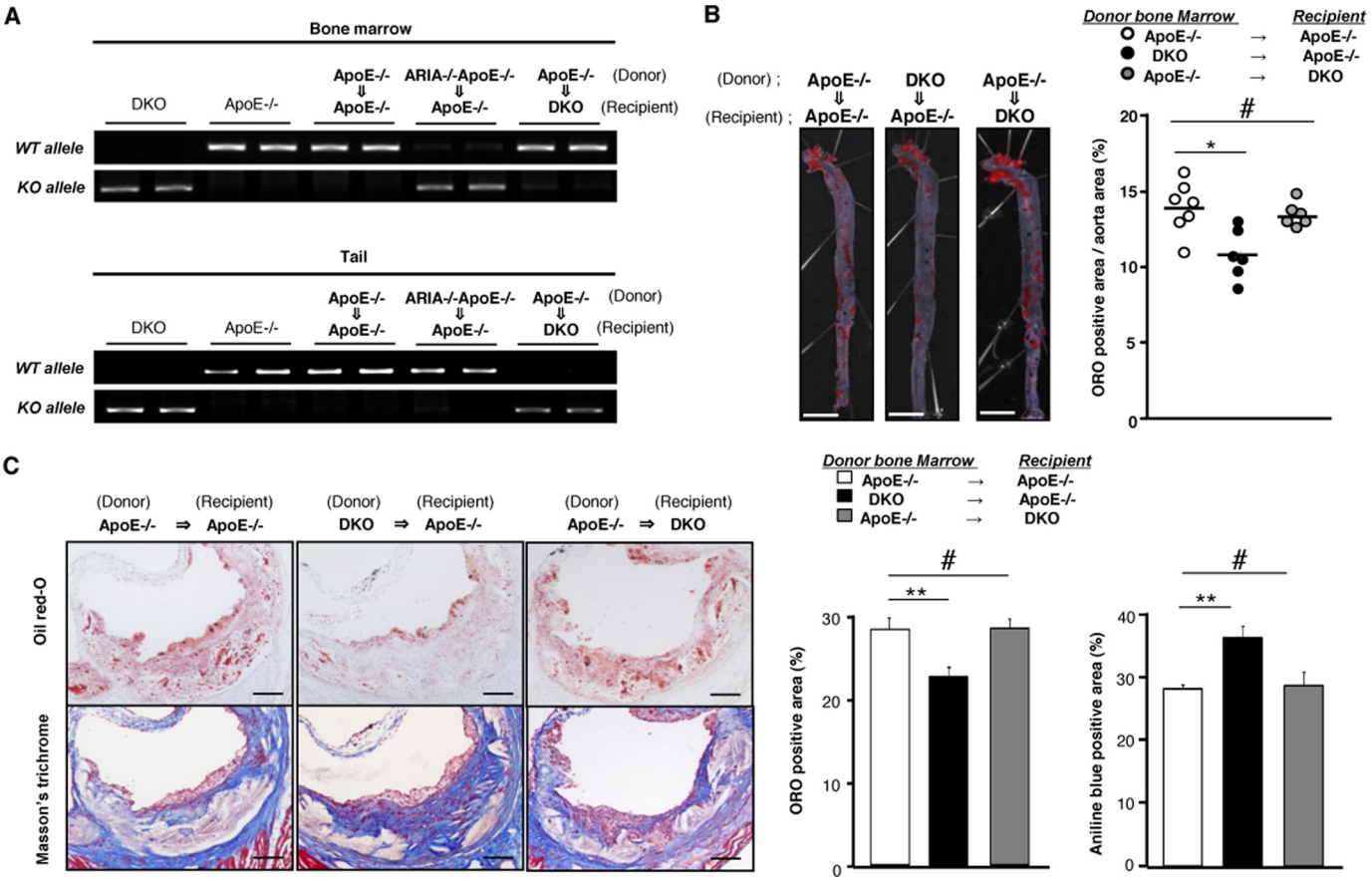

FIGURE 5. **Loss of ARIA in bone marrow cells is sufficient to exert anti-atherogenic effects.** *A*, successful bone marrow transplantation was confirmed by genotyping of bone marrows and tails of recipient mice. *B*, en face preparation of the aorta stained with oil red-O (*ORO*). ApoE$^{-/-}$ (ARIA$^{+/+}$) mice transplanted with DKO bone marrows showed significantly reduced atherosclerosis as compared with control ApoE$^{-/-}$ mice transplanted with ApoE$^{-/-}$ bone marrows. *, $p < 0.05$ and #, NS ($n = 6$ each). In contrast, DKO mice transplanted with ApoE$^{-/-}$ (ARIA$^{+/+}$) bone marrow exhibited atherosclerotic lesion similar to control mice. *Bar*: 5 mm. *C*, histology of plaques at the aortic sinus stained with oil red-O or Masson's trichrome. ApoE$^{-/-}$ (ARIA$^{+/+}$) mice transplanted with DKO bone marrows showed significantly reduced oil red-O-positive lipid-rich area as compared with control ApoE$^{-/-}$ mice transplanted with ApoE$^{-/-}$ bone marrows. **, $p < 0.01$ ($n = 6$ each). Also, ApoE$^{-/-}$ (ARIA$^{+/+}$) mice transplanted with DKO bone marrows showed significantly increased collagen content as compared with control mice. **, $p < 0.01$ ($n = 6$ each). In contrast, DKO mice transplanted with ApoE$^{-/-}$ (ARIA$^{+/+}$) bone marrows exhibited oil red-O-positive lipid-rich area and collagen content similar to control mice. #, NS ($n = 6$ each). *Bar*: 100 μm. *Error bars* in *C* indicate mean ± S.E.

ACAT-1 expression in macrophages. ARIA-mediated modification of ACAT-1 expression altered foam cell formation, and ARIA$^{-/-}$ mice exhibited significant reduction of atherosclerotic lesion formation *in vivo*. These results indicate that ARIA is involved in the physiological and/or pathological regulation of ACAT-1 expression in macrophages and thus modulates their foam cell formation.

The protective role of Akt1 in atherosclerosis has also been reported (17). Similar to Akt3-deficient mice, Akt1-deficient mice developed severe atherosclerosis and occlusive coronary artery disease. However, in contrast to Akt3, bone marrow transplantation experiments revealed that the vascular origin, but not the macrophage origin, of Akt1 exerts vascular protection against atherosclerosis. Akt1 and Akt3 have different roles in macrophages, presumably because of their different subcellular localization (18). ARIA negatively regulates PI3K function by increasing membrane association of PTEN (20). Because PI3K is an upstream activator of Akt1 and Akt3, ARIA probably modulates their activities in endothelial cells and macrophages. However, analysis of bone marrow chimeric mice demonstrated that macrophage-derived but not vascular-derived ARIA significantly contributes to the progression of atherosclerosis. Although vascular Akt plays a crucial role in protecting blood vessels from atherosclerosis, it remains unclear whether enhancing vascular Akt exerts further protection against atherogenesis. Moreover, loss of ARIA induced a moderate increase in Akt activity of ~2-fold in endothelial cells (20); therefore, more accentuation of Akt activity might be necessary to exert further protective effects on atherosclerosis. In contrast, loss of ARIA in BMCs significantly reduced atherosclerosis, suggesting that the moderate activation of Akt in macrophages (~2.5-fold) by ARIA deletion might be sufficient to exert atheroprotective effects. However, we cannot exclude the possibility that bone marrow-derived cells other than macrophages, *e.g.* T-lymphocytes, play a significant role in the inhibition of atherosclerogenesis induced by ARIA deletion (26). Further analysis, including determining the potential expression and role of ARIA in T cells, is required to elucidate the detailed molecular mechanism underlying the ARIA-mediated modification of atherosclerosis.

Our data revealed a previously unknown role of ARIA in the progression of atherosclerosis. Because the atheroprotective effect of ARIA deletion appeared to be attributed to a reduction in macrophage foam cell formation, inhibition of ARIA might

prevent atherosclerosis independent of the control of risk factors such as hyperlipidemia and hyperglycemia. Moreover, we have previously demonstrated that loss of ARIA enhanced insulin sensitivity, as well as protected mice from diet-induced obesity and metabolic disorders by modulating endothelial insulin signaling and adipose tissue angiogenesis (27). Additionally, genetic loss of ARIA ameliorated doxorubicin-induced cardiomyopathy (21). These findings strongly suggest that ARIA is a unique and distinctive target for the prevention and/or treatment of cardiovascular diseases. However, further investigation is required to prove its feasibility as a therapeutic target because ARIA regulates angiogenesis, which has a significant role in tumor growth as well.

Acknowledgment—We thank Yuka Soma for excellent technical assistance.

REFERENCES

1. Thompson, R. C., Allam, A. H., Lombardi, G. P., Wann, L. S., Sutherland, M. L., Sutherland, J. D., Soliman, M. A., Frohlich, B., Mininberg, D. T., Monge, J. M., Vallodolid, C. M., Cox, S. L., Abdel-Maksoud, G., Badr, I., Miyamoto, M. I., Nureldin, A. H., Narula, J., Finch, C. E., and Thomas, G. S. (2013) Atherosclerosis across 4000 years of human history: the Horus study of four ancient populations. *Lancet* **381,** 1211–1222
2. Lusis, A. J. (2000) Atherosclerosis. *Nature* **407,** 233–241
3. Faxon, D. P., Creager, M. A., Smith, S. C., Jr., Pasternak, R. C., Olin, J. W., Bettmann, M. A., Criqui, M. H., Milani, R. V., Loscalzo, J., Kaufman, J. A., Jones, D. W., and Pearce, W. H., (2004) Atherosclerotic Vascular Disease Conference: Executive summary: Atherosclerotic Vascular Disease Conference proceeding for healthcare professionals from a special writing group of the American Heart Association. *Circulation* **109,** 2595–2604
4. Linton, M. F., and Fazio, S. (2003) Macrophages, inflammation, and atherosclerosis. *Int. J. Obes. Relat. Metab. Disord.* **27,** Suppl. 3, S35–S40
5. Moore, K. J., and Tabas, I. (2011) Macrophages in the pathogenesis of atherosclerosis. *Cell* **145,** 341–355
6. Shashkin, P., Dragulev, B., and Ley, K. (2005) Macrophage differentiation to foam cells. *Curr. Pharm. Des.* **11,** 3061–3072
7. Yuan, Y., Li, P., and Ye, J. (2012) Lipid homeostasis and the formation of macrophage-derived foam cells in atherosclerosis. *Protein Cell* **3,** 173–181
8. Yagyu, H., Kitamine, T., Osuga, J., Tozawa, R., Chen, Z., Kaji, Y., Oka, T., Perrey, S., Tamura, Y., Ohashi, K., Okazaki, H., Yahagi, N., Shionoiri, F., Iizuka, Y., Harada, K., Shimano, H., Yamashita, H., Gotoda, T., Yamada, N., and Ishibashi, S. (2000) Absence of ACAT-1 attenuates atherosclerosis but causes dry eye and cutaneous xanthomatosis in mice with congenital hyperlipidemia. *J. Biol. Chem.* **275,** 21324–21330
9. Fazio, S., Major, A. S., Swift, L. L., Gleaves, L. A., Accad, M., Linton, M. F., and Farese, R. V., Jr. (2001) Increased atherosclerosis in LDL receptor-null mice lacking ACAT1 in macrophages. *J. Clin. Invest.* **107,** 163–171
10. Perrey, S., Legendre, C., Matsuura, A., Guffroy, C., Binet, J., Ohbayashi, S., Tanaka, T., Ortuno, J. C., Matsukura, T., Laugel, T., Padovani, P., Bellamy, F., and Edgar, A. D. (2001) Preferential pharmacological inhibition of macrophage ACAT increases plaque formation in mouse and rabbit models of atherogenesis. *Atherosclerosis* **155,** 359–370
11. Bocan, T. M., Krause, B. R., Rosebury, W. S., Mueller, S. B., Lu, X., Dagle, C., Major, T., Lathia, C., and Lee, H. (2000) The ACAT inhibitor avasimibe reduces macrophages and matrix metalloproteinase expression in atherosclerotic lesions of hypercholesterolemic rabbits. *Arterioscler. Thromb. Vasc. Biol.* **20,** 70–79
12. Ikenoya, M., Yoshinaka, Y., Kobayashi, H., Kawamine, K., Shibuya, K., Sato, F., Sawanobori, K., Watanabe, T., and Miyazaki, A. (2007) A selective ACAT-1 inhibitor, K-604, suppresses fatty streak lesions in fat-fed hamsters without affecting plasma cholesterol levels. *Atherosclerosis* **191,** 290–297
13. Farese, R. V., Jr. (2006) The nine lives of ACAT inhibitors. *Arterioscler. Thromb. Vasc. Biol.* **26,** 1684–1686
14. Kharbanda, R. K., Wallace, S., Walton, B., Donald, A., Cross, J. M., and Deanfield, J. (2005) Systemic Acyl-CoA:cholesterol acyltransferase inhibition reduces inflammation and improves vascular function in hypercholesterolemia. *Circulation* **111,** 804–807
15. Tardif, J. C., Grégoire, J., L'Allier, P. L., Anderson, T. J., Bertrand, O., Reeves, F., Title, L. M., Alfonso, F., Schampaert, E., Hassan, A., McLain, R., Pressler, M. L., Ibrahim, R., Lespérance, J., Blue, J., Heinonen, T., Rodés-Cabau, J, and the Avasimibe and Progression of Lesions on UltraSound (A-PLUS) Investigators. (2004) Effects of the acyl coenzyme A:cholesterol acyltransferase inhibitor avasimibe on human atherosclerotic lesions. *Circulation* **110,** 3372–3377
16. Nissen, S. E., Tuzcu, E. M., Brewer, H. B., Sipahi, I., Nicholls, S. J., Ganz, P., Schoenhagen, P., Waters, D. D., Pepine, C. J., Crowe, T. D., Davidson, M. H., Deanfield, J. E., Wisniewski, L. M., Hanyok, J. J., and Kassalow, L. M. and the ACAT Intravascular Atherosclerosis Treatment Evaluation (ACTIVATE) Investigators (2006) Effect of ACAT inhibition on the progression of coronary atherosclerosis. *N. Engl. J. Med.* **354,** 1253–1263
17. Fernández-Hernando, C., Ackah, E., Yu, J., Suárez, Y., Murata, T., Iwakiri, Y., Prendergast, J., Miao, R. Q., Birnbaum, M. J., and Sessa, W. C. (2007) Loss of Akt1 leads to severe atherosclerosis and occlusive coronary artery disease. *Cell Metab.* **6,** 446–457
18. Ding, L., Biswas, S., Morton, R. E., Smith, J. D., Hay, N., Byzova, T. V., Febbraio, M., and Podrez, E. A. (2012) Akt3 deficiency in macrophages promotes foam cell formation and atherosclerosis in mice. *Cell Metab.* **15,** 861–872
19. Ikeda, K., Nakano, R., Uraoka, M., Nakagawa, Y., Koide, M., Katsume, A., Minamino, K., Yamada, E., Yamada, H., Quertermous, T., and Matsubara, H. (2009) Identification of ARIA regulating endothelial apoptosis and angiogenesis by modulating proteasomal degradation of cIAP-1 and cIAP-2. *Proc. Natl. Acad. Sci. U.S.A.* **106,** 8227–8232
20. Koide, M., Ikeda, K., Akakabe, Y., Kitamura, Y., Ueyama, T., Matoba, S., Yamada, H., Okigaki, M., and Matsubara, H. (2011) Apoptosis regulator through modulating IAP expression (ARIA) controls the PI3K/Akt pathway in endothelial and endothelial progenitor cells. *Proc. Natl. Acad. Sci. U.S.A.* **108,** 9472–9477
21. Kitamura, Y., Koide, M., Akakabe, Y., Matsuo, K., Shimoda, Y., Soma, Y., Ogata, T., Ueyama, T., Matoba, S., Yamada, H., and Ikeda, K. (2014) Manipulation of cardiac phosphatidylinositol 3-kinase (PI3K)/Akt signaling by apoptosis regulator through modulating IAP expression (ARIA) regulates cardiomyocyte death during doxorubicin-induced cardiomyopathy. *J. Biol. Chem.* **289,** 2788–2800
22. Xu, S., Huang, Y., Xie, Y., Lan, T., Le, K., Chen, J., Chen, S., Gao, S., Xu, X., Shen, X., Huang, H., and Liu, P. (2010) Evaluation of foam cell formation in cultured macrophages: an improved method with Oil Red O staining and DiI-oxLDL uptake. *Cytotechnology* **62,** 473–481
23. Rodriguez, A., Bachorik, P. S., and Wee, S. B. (1999) Novel effects of the acyl-coenzyme A:cholesterol acyltransferase inhibitor 58-035 on foam cell development in primary human monocyte-derived macrophages. *Arterioscler. Thromb. Vasc. Biol.* **19,** 2199–2206
24. Nakagawa, Y., Ikeda, K., Akakabe, Y., Koide, M., Uraoka, M., Yutaka, K. T., Kurimoto-Nakano, R., Takahashi, T., Matoba, S., Yamada, H., Okigaki, M., and Matsubara, H. (2010) Paracrine osteogenic signals via bone morphogenetic protein-2 accelerate the atherosclerotic intimal calcification *in vivo*. *Arterioscler. Thromb. Vasc. Biol.* **30,** 1908–1915
25. Shimoda, Y., Matsuo, K., Ono, K., Soma, Y., Ueyama, T., Matoba, S., Yamada, H., and Ikeda, K. (2014) Aging differentially alters the expression of angiogenic genes in a tissue-dependent manner. *Biochem. Biophys. Res. Commun.* **446,** 1243–1249
26. Daugherty, A., and Rateri, D. L. (2002) T lymphocytes in atherosclerosis: the yin-yang of Th1 and Th2 influence on lesion formation. *Circ. Res.* **90,** 1039–1040
27. Akakabe, Y., Koide, M., Kitamura, Y., Matsuo, K., Ueyama, T., Matoba, S., Yamada, H., Miyata, K., Oike, Y., and Ikeda, K. (2013) Ecscr regulates insulin sensitivity and predisposition to obesity by modulating endothelial cell functions. *Nat. Commun.* **4,** 2389